CHAPTER 5

Ligand induced symmetry breaking and concomitant blue shift of emission wavelength in octahedral chromium complex

Abstract

The fifth chapter deals with designing of efficient luminescent materials based on octahedral hexaaminechromium(III) complex. It is found that distortion of the octahedral symmetry of $[Cr^{III}(NH_3)_6]^{3+}$ by replacing the axial ligands with weaker halides influences the stability of the doublet state with respect to the quartet ground state. This replacement affects the doublet to quartet transition responsible for phosphorescence. The relative positions of the halides and ammonia in the spectrochemical series play an important role in the tuning of emission wave length. The proximity of fluorine and ammonia in the spectrochemical series causes blue-shift in the emission wavelength and thus provides a rational way for designing blue emitting phosphorescent materials, essential in OLED application for full color display.

5.1. Introduction

Luminescent materials have attracted considerable interest[239-241] due to their multifarious applications in organic light emitting diodes (OLEDS),[47, 242, 243] light emitting electrochemical cells (LEECS),[244] light absorbers in dye-sensitized solar cells,[245, 246] chemosensors, biosensors,[247, 248] lumophores for cell imazing, [249, 250] chemical photo catalysts,[251, 252] and so on. The suitability of luminescent materials for a specific application depends upon the stability of the system, color purity of the emitted light, high emission quantum yield, specific emission decay time and several other factors. In last decades, considerable efforts have been put in the quest of highly efficient emitters with three primary colors (red, green and blue), which are essential for full-color display. Although, red and green light emitting transition metal complexes are abundant due to triplet harvesting,[253, 254] blue light emitting phosphorescent materials are not easily available for the requirement of wide energy gap between the excited and the ground state.[255] The strong spin-orbit coupling (SOC) in the organometallic complexes containing heavy transition metals weakens the spin forbiddenness of transitions between the ground and the excited states and thus these systems partially fulfill the criteria of an ideal luminescent material.[256] However, the dd^* transitions in heavy metals largely quench the luminescence of blue phosphorescent materials.[257, 258] Another difficulty with heavy metals is the triplet-triplet annihilation which hinders the process of phosphorescence and in turn makes the materials unfit for OLED application.[254, 259] To surmount these difficulties with heavy metals, the *3d* transition metal complexes are the best alternative. For example, recently a Cu (I) complex have been found to be a blue emitter (λ_{max}= 436nm) by Yersin et al.,[260] though it's emission decay time is still too long for high brightness OLED application. Hamada et al. reported some Zn (II) complexes as greenish white emitter as well.[261] However, among the *3d* transition metal complexes, the Cr (III) systems have emerged as efficient luminescent materials for their substantial quantum yield and possibility of both the emission processes (fluorescence and phosphorescence) in liquid media at room temperature.[59, 262] Though, there exists sufficient number of experimental reports on the photoresponsive behavior of Cr (III) complexes, a comprehensive theoretical account of the phosphorescence in octahedral (O_h) Cr (III) complex is still awaited. All these facts inspire the selection of octahedral Cr (III) complex for the theoretical investigation of its luminescent property.

The present work is divided into two parts. In the first part, a hexa-amine Cr (III) system is opted for the theoretical investigation of its luminescent property. Subsequently, the absorption

and emission wavelengths of the chosen system are computed and the values are compared with the experimental data to standardize the computational methodology. The octahedral Cr (III) complexes are found to exhibit fluorescence with weak ligands like F^-, Cl^-, Br^- and phosphorescence with strong ligands such as carbonyl, ammonia, cyano etc.[262] However, literature survey reveals the dearth of blue-emitting Cr (III) complexes compared to the red- or green-emitters. These facts form the basis of the second part of the work where we put our effort to find out the appropriate set of ligands which can induce the blue-shift in the emission wave length. The phosphorescence in O_h Cr (III) complex involves excitation from ground state quartet (Q) to excited state quartet (Q') followed by intersystem crossing (ISC) to the doublet state (D). The phosphorescence energy thus depends on the separation between the lowest doublet (D) and the quartet ground state (Q) which is nearly equal to the absorption energy due to $Q \rightarrow D$ transition.[262] Hence, in principle, the excitation of the doublet state compared to the quartet ground state can lead to the blue shift in the emission wave length. The doublet state in the O_h Cr (III) complex can be realized by lifting the degeneracy of the t_{2g} states. In order to do so, the symmetry of the O_h $[Cr^{III}(NH_3)_6]^{3+}$ complex is disturbed by replacing the axial ammonia with the weak halides (I^-, Br^-, Cl^- and F^-). Thus, imposing the asymmetry to the complex through axial ligand substitution in $[Cr^{III}(NH_3)_6]^{3+}$, the doublet state can be induced. Putting different halogens in the axial position, a trend in the change of emission wave length is observed in order to achieve the blue-shift. This study may provide a useful guideline in rational design of metal complexes with desired degree of luminescence behavior and more specifically blue-emitting phosphorescence.

5.2. Computational Methods

For the geometry optimization of the studied complexes at their ground state, the B3PW91 functional is employed. This functional works well for the transition metals and has been successfully employed for studying the photo-physical properties.[263, 264] However, to check the performance of other functional, we had also done the same set of calculations with the most popular GGA functional PBE and meta-GGA functional TPSS. However, since the hybrid-GGA functional is placed higher than pure GGA functional in the Jacob's ladder of Perdew because of its ability to partially minimize the self-interaction energy, we present the B3PW91 result in the main text and for comparison PBE and TPSS results are provided in the supplementary. Hay and Wadt's double-zeta effective core potential (LANL2DZ) is chosen as the basis set for all the computations.[265, 266] Since the phosphorescence of the systems under investigation involves the

quartet and doublet spin states, unrestricted formalism is adopted in the density functional theory (DFT) calculations. The absorption and emission energies of the reference systems are obtained through the time dependent DFT (TDDFT) method coupled with same exchange-correlation functional and basis set as applied for geometry optimization of the ground quartet (*Q*) and doublet (*D*) states. The TDDFT approach offers a reliable route for the calculation of vertical electronic excitation spectra.[267, 268] This fact is supported by the good agreement of experimental spectral property with TDDFT results obtained for transition-metal complexes.[269, 270] Although solvent plays important role in determining excitation values. We have calculated the energy values for different energy states (quartet, doublet, excited quartet) of $[Cr^{III}(NH_3)_6]^{3+}$ complex and found these states are minutely stabilized compared to the gas phase calculation. Hence in order to reduce the computational rigors we rely on the gas phase calculations. However, to get the accurate description of the excited quartet state (*Q′*) of all the reference systems, we resort to more sophisticated complete active space self consistent field (CASSCF) method with an active space of (3, 5) and LANL2DZ basis set. With the initial guess from the state average calculation, the final geometry of the excited quartet state is obtained. Next, a single point calculation at the same DFT level is performed on this optimized geometry of the excited state molecules for comparison with the ground state condition obtained in the level of DFT. In every case, vibrational analysis is performed at the same DFT level to assure the structural stability of the systems. All the computations were done with the GAUSSIAN09W suit of quantum chemical package.[142]

5.3. Results and discussions

The structural parameters and energies of the optimized geometries of $[Cr^{III}(NH_3)_6]^{3+}$ in its quartet ground state (*Q*), quartet excited state (*Q′*) and the lowest energy doublet state (*D*) are given in the Table 1. In the quartet ground state, all the Cr-$(NH_3)_6$ bond lengths are found to be equal, which ascertains the O_h symmetry of the system. The molecular orbital (MO) analysis in the quartet ground state reveals that the highest occupied molecular orbital (HOMO) and next two orbitals (HOMO – 1 and HOMO – 2) are composed with maximum contribution from Cr *d*-orbitals *viz.,* d_{xz}, d_{yz} and d_{xy}. On the other hand, the lowest unoccupied molecular orbital (LUMO) and the LUMO + 1 orbitals are mainly constituted by the Cr d_{z^2} and $d_{x^2-y^2}$ orbitals (Figure 5.1). Thus, in the octahedral field the splitting of the Cr MOs into t_{2g} and e_g set of orbitals can be confirmed in this $[Cr^{III}(NH_3)_6]^{3+}$ complex (Figure 5.1).

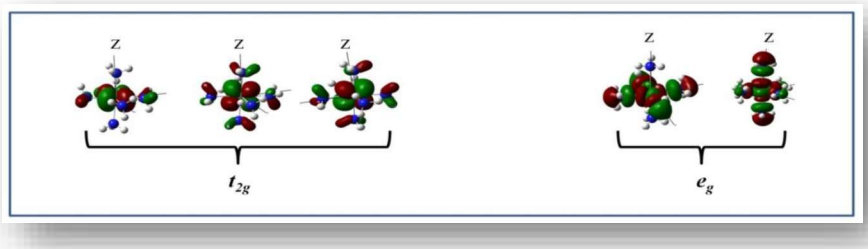

Figure 5.1. *t_{2g} and e_g set of orbitals in $[Cr^{III}(NH_3)_6]^{3+}$.*

From the analysis of the TDDFT computation, carried out on the ground quartet state of $[Cr^{III}(NH_3)_6]^{3+}$, the leading excitations occurs at 420 nm (Table 5.2), which is quite close to the experimental value of absorption wavelength (Table 5.2).[262] The major contribution to this absorption energy comes from the electronic excitation from the 37th up-spin occupied orbital (α-HOMO) to the initially unoccupied 38th α-LUMO [Table S1(a) in Supporting Information]. Thus, the excited quartet state (Q') acquires the electronic configuration $t_{2g}^2\ e_g^1$ due to spin reserved electron excitation from t_{2g} to e_g level. The electronic configuration $t_{2g}^2\ e_g^1$ in the excited quartet state is supported from the elongation in the distance between Cr and equatorial ligands compared to the quartet ground state (Q) (Table 5.1). In the excited quartet state, the 38th α-MO which is primarily composed of the Cr $d_{x^2-y^2}$ orbital, gets populated due to electronic excitation and the presence of electron in Cr $d_{x^2-y^2}$ orbital causes the elongation in the equatorial (xy) plane. On the contrary, the axial Cr-(NH_3) distance remains almost unaltered in the ground and excited quartet states of the molecule (Table 5.1). Unlike the excited quartet state, the geometry in the doublet state is not much distorted compared to the ground state quartet (Table 5.1). In the doublet state the electronic distribution alters within the d_{xy}, d_{yz} and d_{zx} set of orbitals which are not directly oriented towards the ligands and thus the structural change in the doublet state is nominal with respect to the ground state quartet (Table 5.1).

Table 5.1. *Bond distance between Cr and axial ligand (Cr-L_{ax}), Cr and equatorial ligand (Cr-L_{eq}) and energies of the $[Cr^{III}(NH_3)_6]^{3+}$ at quartet ground state (Q), quartet excited state (Q´), and doublet ground state (D).*

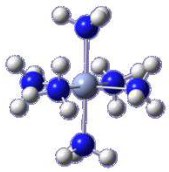

States	Cr-L_{ax} (Å)	Cr-L_{eq} (Å)	Relative energy (Kcal/mol)
Q	2.16	2.16	0
Q´	2.11	2.29	9.41
D	2.13	2.13	28.2

Next, to understand the mechanism of the intersystem crossing between the excited quartet (Q') and doublet state (D), the vibrational modes in both the states are closely observed. After a thorough analysis of the vibrational modes, the 20th mode of Q' (vibrational energy = 379 cm^{-1}) and 16th mode of the D state (vibrational energy = 318 cm^{-1}), are found to have oscillation vectors in the same direction (Figure 5.2). The proximity in the energy and the oscillation pattern in these two vibrational modes suggest that the doublet and the excited quartet states may switch into one another through the vibration as shown in Figure 5.2. From the TDDFT computation on the lowest energy doublet state, the emission wavelength for the $D \rightarrow Q$ transition is obtained as 877 nm, comparable to the experimental value of phosphorescence (Table 5.2).[262] After standardizing the computational framework for the estimation of absorption and emission wavelength, we move to the next part of this work which is carried out in the same computational methodology.

Table 5.2. *Comparison of absorption and emission wavelengths in nm (energies in cm^{-1}) with experimental value in $[Cr^{III}(NH_3)_6]^{3+}$.*

	Computational value	Experimental Value[262]
Absorption($Q \rightarrow Q'$)	420 nm (23804 cm^{-1})	21550 cm^{-1}
Emission ($D \rightarrow Q$)	877 nm (11403 cm^{-1})	15120 cm^{-1}

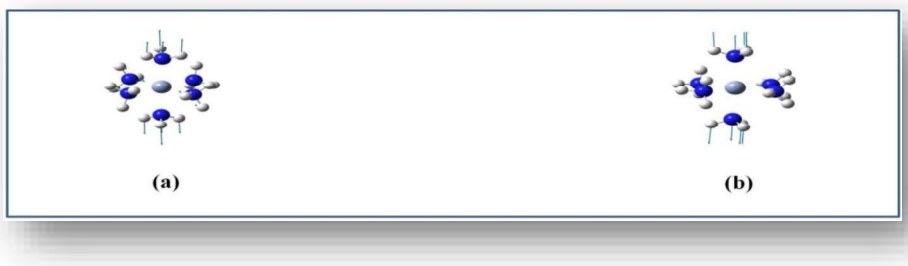

Figure 5.2. *Oscillation vectors in the (a) 16th vibrational modes in the D state and (b) the 20th vibrational mode in the Q′ state of $[Cr^{III}(NH_3)_6]^{3+}$.*

According to the plan discussed in the introduction, the axial ligands in the $[Cr^{III}(NH_3)_6]^{3+}$ are substituted by the weaker halogens to destroy the O_h symmetry of the complex. This is expected to lift the degeneracy of singly occupied t_{2g} orbitals as shown in Figure 5.3 and induce the doublet state in case the axial and equatorial ligands differ sufficiently in strength according to their position in the spectrochemical series. Table 5.3 displays the structural

parameters of the optimized geometry, and energies of all the halogen substituted octahedral Cr (III) complexes.

Table 5.3. *Bond distance between Cr and axial ligand (Cr-L_{ax}), Cr and equatorial ligand (Cr-L_{eq})_and energies of the complex $[Cr^{III}(NH_3)_4(X)_2]^+$ (X= I^-, Br^-, Cl^-, and F^-, represented by violet, brown, green and light blue colors respectively).*

Systems	Electronic States	Cr-L_{ax} (Å)	Cr-L_{eq} (Å)	Relative energy (Kcal/mol)
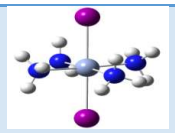 $[Cr^{III}(NH_3)_4(I)_2]^+$	*Q*	2.71	2.12	0
	Q´	2.76	2.28	18.2
	D	2.69	2.11	27.6
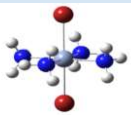 $[Cr^{III}(NH_3)_4(Br)_2]^+$	*Q*	2.51	2.11	0
	Q´	2.56	2.32	10.04
	D	2.46	2.13	11.3
 $[Cr^{III}(NH_3)_4(Cl)_2]^+$	*Q*	2.32	2.10	0
	Q´	2.37	2.34	11.4
	D	2.28	2.12	26.35
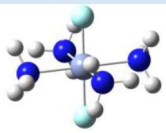 $[Cr^{III}(NH_3)_4(F)_2]^+$	*Q*	1.85	2.11	0
	Q´	1.83	2.27	10.7
	D	1.80	2.12	38.9

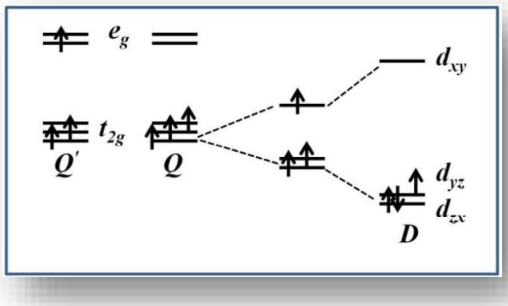

Figure 5.3. *Orbital splitting pattern in the ground state quartet (Q), excited state quartet (Q´), and the doublet state of $[Cr^{III}(NH_3)_6]^{3+}$.*

In the quartet ground state (*Q*), the diiodo, dibromo and dichloro substituted complexes are found to be destabilized compared to the $[Cr^{III}(NH_3)_6]^{3+}$, whereas the difluoro complex is relatively stabilized (Table 5.1 and Table 5. 3). The bond distance between the metal and the apical ligand (Cr-L_{ax}) provides the explanation for such an observation. For the first three

substituted complexes, the Cr-L_{ax} distance is larger than that in the $[Cr^{III}(NH_3)_6]^{3+}$ whereas for the $[Cr^{III}(NH_3)_4F_2]^{+}$, the Cr-$L_{ax}$ distance is much shorter than that in the $[Cr^{III}(NH_3)_6]^{3+}$(Table 5.1 and Table 5.3). Hence, in the present case the bonding between the Cr and axial ligands contributes significantly towards the stability of the halogen substituted complexes. In the excited quartet state (Q') of all the halogen substituted complexes, the bond distances in the equatorial (xy) plane are found to be stretched compared to the quartet ground (Q) state with little variation in the Cr-L_a bond distance. The bond stretching in the xy plane of the Q' state compared to the Q state of these new complexes is attributed to the electronic excitation in the $d_{x^2-y^2}$ orbital similar to the case of $[Cr^{III}(NH_3)_6]^{3+}$. Moreover for stability issue, we calculated hardness of the ground state for all the studied complexes and results are given in tabular form.

Table 5.4. *Calculated hardness values in eV for the studied complex (ground state quartet).*

Systems	Hardness (eV)
$[Cr^{III}(NH_3)_6]^{3+}$	3.34
$[Cr^{III}(NH_3)_4(F)_2]^{+}$	2.37
$[Cr^{III}(NH_3)_4(Cl)_2]^{+}$	2.2
$[Cr^{III}(NH_3)_4(Br)_2]^{+}$	2.18
$[Cr^{III}(NH_3)_4(I)_2]^{+}$	1.15

From the Table 5.4 it can be concluded that among the halide substituted systems, $[Cr^{III}(NH_3)_4(F)_2]^{+}$ is found to be the most stable as maximum hardness means maximum stability.[271] From the TDDFT computation on the quartet ground states of the halogen substituted complexes, the lowest transition is found to take place from α-occupied HOMO (35^{th} α-MO for diiodo, dibromo and dichloro substituted complexes and 37^{th} α-MO for the difluoro substituted complex) to the initially unoccupied LUMO (36^{th} α-MO for diiodo, dibromo and dichloro substituted complexes and 38^{th} α-MO for the difluoro substituted complex) as can be found from Table S1 and Figure S1 in supplementary data. The absorption wavelengths of all the halogen substituted complexes are given in Table 5.5. For these complexes also, the HOMO to HOMO – 2 and LUMO to LUMO + 1 belong to the t_{2g} and e_g set of orbitals as in case for $[Cr^{III}(NH_3)_6]^{3+}$ [Figure S1 (a) – S1 (h) in the Supporting Information]. In all the halogen-substituted complexes the possibility of intersystem crossing between the excited quartet state and doublet state is verified

by the common mode of vibrations of compatible energies in both the spin states [Table S2 in the Supporting Information].

Table 5.5. *Comparison of absorption and emission wavelengths in nm (energies in cm^{-1}) in $[Cr^{III}(NH_3)_4(X)_2]^+$ (X= I^-, Br^-, Cl^-, and F^-).*

Complex	Absorption($Q \rightarrow Q'$)	Emission($D \rightarrow Q$)
$[Cr^{III}(NH_3)_4I_2]^+$	618.4(16171)	1280.7 (7808)
$[Cr^{III}(NH_3)_4Br_2]^+$	554.9(18021)	1416.4 (7060)
$[Cr^{III}(NH_3)_4Cl_2]^+$	502.2(19912)	968 (10331)
$[Cr^{III}(NH_3)_4F_2]^+$	555.4(18004)	453.8 (22036)

From the TDDFT computation on the doublet state, the ligands are found to regulate the emission frequency in the halogen substituted complexes. In the viewpoint of application, the most appealing fact has been the trend in the variation of emission wave length, which can be explained by the relative positions of the halogens in the spectrochemical series. The I^- and Br^- are the weak ligands and hence in stark contrast with the strong ammonia ligand. Thus placing the weak ligand along the *z*-axis, the d_{xz} and d_{yz} orbitals can be stabilized compared to the d_{xy} orbital and hence the threefold degeneracy of the t_{2g} level is lifted (Figure 5.3). This further splitting of the t_{2g} level stabilizes the doublet state compared to the quartet ground state resulting low energy emission as can be confirmed from Table 5.5. Hence, replacement of the axial ligands in $[Cr^{III}(NH_3)_6]^{3+}$ with weak I^- and Br^- causes red shift in the emission wave length. This is further interesting to note that the nearly equal emission wave lengths in the diiodo and dibromo complexes correspond well with their proximate position in the spectrochemical series. Compared to these two complexes, in the difluoro compound the blue shift in the emission wave length is observed with respect to the O_h $[Cr^{III}(NH_3)_6]^{3+}$ complex. This fact can again be explained on the basis of relative strength of axial and equatorial ligands. Among the halogens, the F^- is closest to the ammonia in the spectrochemical series, for which the asymmetry in the t_{2g} is least imposed and the doublet state becomes less favored. This fact increases the energy gap between the doublet and quartet ground state and is reflected in the maximum value of the emission frequency. In alignment with this explanation, in the chloro-substituted complex, the emission wave length is in between that shown by the $[Cr^{III}(NH_3)_4F_2]^+$ and $[Cr^{III}(NH_3)_4I_2]^+$ or $[Cr^{III}(NH_3)_4Br_2]^+$. This trend again matches well with the position of chloride lying between the

I^-, $Br^-$and F^- in the spectrochemical series. In order to see the variation of emission wavelength by replacing ligand other than halide, we include two other ligands, OH^- and CN^-. The former is close to F^- and the later is more separated from F^- in the spectrochemical series. The complex containing stronger ligands, CN^- exhibit emission almost in the same region (676 nm) as $[Cr^{III}(NH_3)_6]^{3+}$, whereas the complex containing OH^- giving red shifted emission (1823 nm).

5.4. Conclusion

In the present work, the photophysical property of an O_h Cr (III) complex is studied in the framework of density functional theory. Primary computational results of the absorption and emission wavelength obtained through TDDFT correspond well with the known phosphorescent behavior of the complex. In the later part, the axial ligands in the O_h $[Cr^{III}(NH_3)_6]^{3+}$ complex is replaced with comparatively weaker ligand so as to disrupt the O_h symmetry of the complex. The weaker ligand along the *z*-axis is expected to stabilize the d_{xz} and d_{yz} orbitals compared to the d_{xy} orbital and thus lifts the degeneracy of the erstwhile t_{2g} set of orbitals. This tetragonal distorted structure brings about electronic redistribution leading to the doublet state as illustrated in the Figure 3. Since, the difference in the strength of the axial and equatorial ligands is the key to further split the degenerate t_{2g} level, we logically replace the axial ligands of O_h $[Cr^{III}(NH_3)_6]^{3+}$ by I^-, Br^-, Cl^-, and F^- which are placed at different positions in the spectrochemical series with respect to NH_3. The propensity of the doublet state is high in the diiodo and dibromo complexes due to large difference in the strength of the I^- and Br^- ligands compared to NH_3. On the contrary, F^- and NH_3 are close in the spectrochemical series. Hence, the doublet state cannot easily be achieved due to equivalent strength of the axial and equatorial ligands. This fact of differing tendency for doublet state due to the variant strength of axial and equatorial ligands is supported by the low energy emission in the diiodo, dibromo complexes and high energy phosphorescence in the fluoro-substituted complex. The position of Cl^- lying between I^-, Br^- and F^- in the spectrochemical series matches well with the emission frequency of the chloro-substituted complex which is also in between the emission frequencies of iodo-, bromo-substituted complexes and fluoro-substituted complex. Thus, here we can see the relative position of the ligands in the spectrochemical series turns effective in tuning the emission frequency of phosphorescence. The most important finding of the present work is the blue-shift in the emission wave-length of $[Cr^{III}(NH_3)_4F_2]^+$. An emission wave length of 454 nm of this complex may offer significant insight for the rational designing of hitherto rare blue-emitting first row transition metal complexes, important for OLED applications.